

The Amyloid Precursor Protein Plays Differential Roles in the UVA Resistance and Proliferation of Human Retinal Pigment Epithelial Cells.

Running title: Differential roles of APP in cellular UVA resistance and proliferation

Fatima Sultan^a and Edward T. Parkin^{*a}

^aDivision of Biomedical and Life Sciences, Faculty of Health and Medicine, Lancaster University, Lancaster, United Kingdom.

*Address correspondence to this author at the Division of Biomedical and Life Sciences, Faculty of Health and Medicine, Lancaster University, Lancaster, United Kingdom. Tel/Fax: +44 1524 592246, +44 1524 593192. E-mail: e.parkin@lancaster.ac.uk

Abstract

Background: Age-related macular degeneration (AMD) can be characterised by degeneration of retinal pigment epithelial (RPE) cells and the accumulation, in retinal drusen deposits, of amyloid beta-peptides proteolytically derived, by secretases, from the amyloid precursor protein (APP). Ultraviolet (UV) light exposure is a risk factor for the development of AMD. **Objectives:** In the current study, we investigated whether APP and/or its proteolysis are linked to the UVA resistance or proliferation of ARPE-19 human RPE cells. **Methods:** Cell viability was determined, following UVA exposure, with prior small interfering RNA-mediated APP depletion or secretase inhibitor treatments. APP levels/proteolysis were analysed by immunoblotting. Cells were also grown in the presence/absence of secretase inhibitors to assess their effects on longer-term culture growth. Finally, the effects of APP proteolytic fragments on ARPE-19 cell proliferation were monitored following co-culture with human embryonic kidney cells stably over-expressing these fragments. **Results:** Endogenous APP was depleted following UVA irradiation and β -secretase, but not α -secretase, processing of the protein was reduced. Experimental APP depletion or γ -secretase (but not α - or β -secretase) inhibition ablated the detrimental effect of UVA on cell viability. In contrast, α -secretase, and possibly γ -secretase but not β -secretase activity, appeared to promote the longer-term proliferation of ARPE-19 cells in the absence of UVA irradiation. **Conclusions:** There are clear but differential links between APP expression/proteolysis and the proliferation and UVA resistance of ARPE-19 cells indicating that the protein should be investigated further in relation to the identification of possible drug targets for the treatment of AMD.

Keywords: Amyloid precursor protein, ultraviolet, resistance, proliferation, retinal, pigment, epithelial

1. INTRODUCTION

Age-related macular degeneration (AMD), a progressive retinal disease, is the leading cause of blindness globally with almost 200 million affected individuals ¹. Given increasing population aging, there are expected to be 288 million people living with the disease by 2040 ². AMD is classified as either non-neovascular (dry/atrophic) or neovascular (wet/exudative) according to specific features of the disease. Dry AMD constitutes 80-85% of all cases and is associated with ‘drusen’ deposits, small specks of yellowish white material, in the macula underneath the retina ³. Accumulation of these deposits leads to the gradual destruction of the retinal pigment epithelium (RPE) and the photoreceptors in the macular region ⁴. This manifests clinically with symptoms of blurred central vision that deteriorates gradually over time ⁵. Wet AMD is less common; it accounts for approximately 15% of AMD cases ⁵. However, the symptoms are severe and progress rapidly which makes it responsible for 90% of acute vision loss due to AMD ⁶. Wet AMD is characterised by abnormal choroidal vessels developing underneath the macula and leaking blood and fluid. This eventually results in the formation of a central fibrous sub-retinal scar leading to a sudden decline in central visual acuity ^{3,4}. A common symptom of wet AMD is straight lines appearing wavy or distorted ⁵.

Whilst the molecular pathology of AMD is not yet fully elucidated, ultraviolet (UV) irradiation is known to cause the production of reactive oxygen species (ROS), damage DNA and induce apoptosis in RPE cells ⁷⁻¹² and, together with blue light, is considered a possible risk factor in the development of the disease ¹³⁻¹⁵ although the evidence is still controversial ¹⁶. Epidemiologic evidence suggests that excessive light exposure is associated with increased risk of AMD ⁷. This is due to photochemical damage by the blue light and short wavelength radiation (UVA radiation of 315-400 nm) that is able to penetrate the eye protective structures into the retina ¹⁷. This induces significant oxidative stress to the RPE and leads to

the formation of lipoprotein aggregates in Bruch's membrane and drusen deposits resulting finally in the destruction of photoreceptors in the macula and AMD development¹⁸.

Particularly the dry form of AMD exhibits some molecular commonality with the neurodegenerative condition Alzheimer's disease (AD), the leading form of dementia caused, arguably, by the accumulation of toxic amyloid beta (A β)-peptides in the afflicted brain¹⁹⁻²¹. In addition to a range of other lipids and proteins, drusen deposits contain A β -peptides²²⁻²⁴ and these proteinaceous components are also associated with key stages in AMD progression and linked to disease aetiology²⁵⁻²⁷. Furthermore, the intraocular injection of mice with A β -peptides induces the accumulation of drusen immunopositive for the peptides and leads to degenerative changes in the retina mimicking AMD-like pathology²⁸. Conversely, it has been shown that knocking down the A β -degrading enzyme, neprilysin, leads to the development of AMD-like pathology in mice including the degeneration of RPE cells and the development of drusen-like deposits²⁶. In addition to their role in dry AMD, A β -peptides may also participate in the development of the wet form of the disease by increasing the expression of vascular endothelial growth factor (VEGF) and decreasing the expression of pigment epithelium-derived factor (PEDF) secreted by RPE cells which acts as a potent antiangiogenic factor²⁹⁻³¹.

A β -peptides are derived from the full-length amyloid precursor protein (FL-APP) through sequential proteolysis by two enzyme activities; β - and γ -secretases (Fig.1)³². The former enzyme, also termed BACE1 (β -site APP-cleaving enzyme 1), cleaves at the N-terminus of the A β region within APP yielding a soluble fragment, soluble APP β (sAPP β) and leaving behind a 99 amino acid C-terminal fragment, CTF β , in the membrane. This latter fragment is then cleaved by the γ -secretase complex to yield the toxic A β -peptides and a transcriptionally active APP intracellular domain (AICD)³³. However, this 'amyloidogenic' pathway is

countered by a reciprocal ‘non-amyloidogenic’ pathway (Fig.1) whereby an α -secretase activity (predominantly A Disintegrin And Metalloproteinase 10; ADAM10³⁴) cleaves between Lys16 and Leu17 in the A β region of APP precluding the formation of intact A β -peptides³⁵. However, it is becoming increasingly apparent that the soluble APP α (sAPP α) fragment generated by α -secretase cleavage of APP, in addition to the preclusion of A β -peptide formation, is of great importance in combatting the neurodegeneration observed in AD³⁶. Specifically, sAPP α has been implicated in neurogenesis, brain development and plasticity³⁶ and the neuroprotective actions of the fragment in vivo include enhancement of neuronal survival, protection from ROS and decreased glutamate-mediated excitotoxicity³⁷⁻

39.

Given the potential aetiological links between A β -peptides, UV and AMD it is perhaps surprising that APP processing and its relationship to UV exposure in RPE cells has not previously been investigated. In the current study, we show that APP expression and proteolysis are altered following UVA exposure in ARPE-19 human retinal pigment epithelial cells. Furthermore, experimental depletion of the protein enhanced cell viability following UVA irradiation. Preventing α - or β -secretase-mediated APP processing did not modify ARPE-19 cell viability following UVA irradiation. However, interestingly, treatment with the notch-sparing APP γ -secretase inhibitor, begacestat, did partly ablate the negative impact of UVA on cell viability. Notably, these effects were distinct from the roles of APP proteolysis in longer-term ARPE-19 cell proliferation where inhibiting α -secretase activity did have a negative impact and sAPP α itself enhanced viable cell numbers. Furthermore, whereas β -secretase inhibition had little effect on longer-term cell proliferation, begacestat negatively impacted on viable cell numbers in this respect. Collectively, these data indicate that APP has important but differential roles in the UVA resistance and proliferation of

human RPE cells and should be investigated further in relation to the identification of possible drug targets for the treatment of AMD.

2. MATERIALS AND METHODS

2.1. Certification of human retinal pigment epithelial (ARPE-19) cells

ARPE-19 cells were purchased from American Type Culture Collection (ATCC; distributed by LGC Standards, Teddington, UK). On receipt, cells were seeded, harvested and then aliquoted into multiple P1 stocks in liquid nitrogen. All experiments were subsequently performed on resurrected cells within five passages of original seeding. The cell line was subjected to short tandem repeat (STR) profile testing by the laboratory analysis service of ATCC. Seventeen short tandem repeat (STR) loci plus the gender determining locus, Amelogenin, were amplified using the commercially available PowerPlex® 18D Kit from Promega (Madison, USA). The cell line sample was processed using the ABI Prism® 3500xl Genetic Analyzer. Data were analyzed using GeneMapper® ID-X v1.2 software (Applied Biosystems, Waltham, USA). Appropriate positive and negative controls were used throughout the test procedure. The DNA profile (STRB7331) was as follows: TH01: 6, 9.3; D5S818: 13; D13S317: 11, 12; D7S820: 9, 11; D16S539: 9, 11; CSF1PO: 11; Amelogenin: X, Y; vWA: 16, 19; TPOX: 9, 11. The ATCC test conclusions were that the submitted sample profile is an exact match for cell line CRL-2302 (ARPE-19) in the ATCC STR database.

2.2. Cell culture

Human embryonic kidney (HEK) cells were generously provided by Professor David Allsop (Lancaster University, Lancaster, UK). Cell culture reagents were purchased from Lonza Ltd. (Basel, Switzerland). ARPE-19 and HEK cells were cultured in Dulbecco's Modified Eagle Medium:F12 (DMEM:F12) and DMEM basal media, respectively, supplemented with 25

mM glucose, 4 mM L-glutamine, 10% (v/v) foetal bovine serum, penicillin (50 U/mL) and streptomycin (50 µg/mL). Cells were maintained at 37°C in 5% CO₂ in air.

For the co-culture experiments a 24-well transwell system containing ThinCert™ cell culture inserts (Greiner Bio One, Stonehouse, UK) was employed. HEK cells (150,000) were seeded in the inserts and ARPE-19 cells (12,250) in the basal wells of the system and, in this instance, both cell types were cultured in DMEM:F12 (supplemented as described above) for seven days before determination of ARPE-19 cell viability.

2.3. Cell treatments

For UVA irradiation, 80% confluent flasks of ARPE-19 cells were pre-incubated for 6 h in UltraMEM™ reduced serum medium and then transferred into phenol red-free DMEM (containing the appropriate secretase inhibitor treatments if required) before being exposed to UVA irradiation at doses of 0-263 kJm⁻² using six Phillips TLR 36W tubes (Starna Ltd, Romford, UK) with cells 8 cm from the light source (maximum irradiation duration of 20 min). Following irradiation, the medium was replaced with fresh UltraMEM™ (plus/minus secretase inhibitors if necessary) and the cells were cultured for a further 18 h prior to further analysis.

The γ -secretase inhibitor begacestat (GSI-953) and β -secretase inhibitor IV were purchased from Tocris (Bristol, UK) and Merck Millipore (Darmstadt, Germany), respectively. Batimastat was purchased from Merck Life Science (Gillingham, UK). All three inhibitors were prepared as concentrated stock solutions in dimethylsulfoxide (DMSO) and added to cell culture medium to achieve the final concentrations described up to a maximum carrier concentration of 0.05% (v/v). All control cultures contained the equivalent carrier concentration.

2.4. Cell viability measurements

Cell viability was determined by Trypan Blue (Merck Life Science) or 3-(4,5-dimethylthiazol-2-yl)-5-(3-carboxymethoxyphenyl)-2-(4-sulfophenyl)-2H-tetrazolium (MTS) (Promega, Madison, USA) analyses according to the manufacturers' instructions.

2.5. Stable transfection of HEK cells

The generation of the full-length APP construct in the mammalian expression vector pIRESHyg (Clontech-Takara Bio Europe, Saint-Germain-en-Laye, France) has been reported previously⁴⁰. The sAPP α and sAPP β constructs were generated by site-directed mutagenesis of the full-length APP-pIRESHyg construct to introduce stop codons after the nucleotides encoding lysine or methionine, respectively, upstream of the α - and β -secretase cleavage sites. Plasmids (30 μ g) or empty expression vector (control cells) were linearized using AhdI before being subjected to ethanol precipitation and subsequent introduction into HEK cells by electroporation. Recombinant cells were selected using 150 μ g/mL hygromycin (Invitrogen, Paisley, UK).

2.6. Small interfering RNA (siRNA) transfection

Smart pool siRNA was purchased from Horizon Discovery Biosciences (Cambridge, UK) and consisted, specifically, of non-targeting #1 siRNA control pool (Cat. No. D-001206-13-05) and human APP targeting siRNA SMARTpool (Cat. No. M-003731-00). ARPE-19 cells (70% confluence) in complete growth medium (but lacking antibiotics) were treated with siRNA which had been pre-complexed with DharmaFECT 1 transfection reagent (Horizon Discovery Biosciences). After 24 h, the growth medium was refreshed and, following a further 24 h, the medium was replaced with phenol red-free DMEM before exposing the cells to UVA.

2.7. Preparation of cell lysates and conditioned medium samples

Conditioned cell culture medium was harvested, centrifuged at 10,000 g for 10 min to remove cell debris, and concentrated 50-fold using Vivaspin 6 centrifugal concentrators (Sartorius, Epsom, UK). For analysis of cell-associated proteins, cells were washed with phosphate-buffered saline (PBS; 20 mM Na₂HPO₄, 2 mM NaH₂PO₄, 0.15 M NaCl, pH 7.4) and scraped from the flasks into fresh PBS (10 mL). Following centrifugation at 500 g for 5 min, cell pellets were lysed in 50 mM Tris, 150 mM NaCl, 1% (v/v) IGEPAL, 0.1 % (w/v) sodium deoxycholate, 5 mM EDTA at pH 7.4 containing protease inhibitor cocktail (Merck Life Science).

2.8. Protein assay, sodium dodecyl sulphate polyacrylamide gel electrophoresis (SDS-PAGE) and immunoblot analysis

Protein levels in cell lysates were quantified using bicinchoninic acid ⁴¹ in a microtitre plate with bovine serum albumin as a standard. Equal quantities of lysate protein and equal volumes of concentrated conditioned medium samples were resolved by SDS-PAGE using 5-20% polyacrylamide gradient gels and transferred to Immobilon P polyvinylidene difluoride (PVDF) membranes ⁴² before incubating with primary antibody. Anti-actin monoclonal and anti-APP C-terminal rabbit polyclonal primary antibodies were from Merck Life Science. Anti-APP 6E10 monoclonal and anti-sAPP β rabbit polyclonal primary antibodies were from Biogen (San Diego, USA). Bound antibody was detected using peroxidase-conjugated secondary antibodies (Merck Life Science) in conjunction with enhanced chemiluminescence detection reagents (Fisher Scientific, Loughborough, UK).

2.9. Statistical analysis

Data are presented as means \pm S.D. and were subjected to statistical analysis via Student's t-test or one-way analysis of variance (ANOVA) with Tukey's post hoc tests. Levels of significance are indicated in figure legends.

2.10. Funding

This research did not have a specific funding source and forms part of the employment of the corresponding author who, as an employee and representative of Lancaster University, was responsible for the writing, editing, approval and decision to publish the article.

3. RESULTS

3.1. Levels of APP and secreted sAPP β but not sAPP α are decreased in ARPE-19 cultures following UVA exposure

As cellular APP levels have previously been shown to decrease in various other cell lines following UV exposure⁴³, we sought to determine whether these observations could be recapitulated in the retinal pigment epithelial cell line, ARPE-19. Initially, we determined an appropriate UVA dose to use for the remainder of the study by exposing 80% confluent cell cultures to doses ranging from 0-263 kJm⁻² and then measuring cell viability after an 18 h recovery period as described in the Materials and Methods section. The results (Fig.2) demonstrated that a 105 kJm⁻² UVA dose induced a moderate 32.1 \pm 1.4 % decrease in viable cell count relative to the control mock-irradiated cell cultures. Higher doses of 158, 210 and 263 kJm⁻² led to more dramatic decreases in viable cell numbers by 79.8 \pm 3.1, 99.8 \pm 0.3 and 100 \pm 0.0 % respectively, relative to controls.

We next examined the effects of a single appropriate UVA dose (105 kJm⁻²) on the levels of APP and its proteolytic fragments in ARPE-19 cell cultures. Lysate samples from UVA- and mock-irradiated cells were subjected to immunoblotting using the anti-APP C-terminal antibody as described in the Materials and Methods section. Various possible isoforms and maturation states of APP were detected (Fig. 3A). Given that ARPE-19 cells are not neuronal cells, it is most likely that the larger band represents the mature forms of APP₇₇₀ and/or

APP₇₅₁ and the lighter band indicates the immature form(s) of these isoforms. Furthermore, the absence of APP₆₉₅ in ARPE-19 cells has previously been confirmed in our laboratory by comparing immunoblot patterns between mock- and APP₆₉₅-transfected ARPE-19 stable transfectants (Parkin et al. unpublished data). Quantification of multiple immunoblots (Fig. 3A) showed that FL-APP levels decreased by 45.9 ± 16.3 % following UVA treatment.

As a measure of amyloidogenic versus non-amyloidogenic APP processing we also quantified the levels of α -secretase derived sAPP α and β -secretase derived sAPP β in conditioned medium from mock- and UVA-irradiated cells. First, the anti-APP 6E10 antibody which recognises amino acid residues 1-16 of the beta amyloid sequence was used in order to detect sAPP α . The results (Fig. 3B) appeared to show that sAPP α levels decreased significantly (by 28.2 ± 15.7 %) following UVA treatment. However, it has to be considered that UVA irradiation resulted in fewer cells in cultures so, in order to obtain a more accurate reflection of the amount of sAPP α secreted 'per cell number', results were corrected in order to account for observed changes in cell viability as determined through trypan blue counting of viable cell numbers (i.e. the immunoblot signals were expressed as a function of viable cell numbers). After doing so (Fig. 3B), sAPP α levels showed no significant difference from the control levels. Second, medium samples were immunoblotted using anti-sAPP β antibody and the results (Fig. 3C) revealed a 51.7 ± 6.8 % decline in sAPP β production following UVA treatment and this decline persisted even after taking viability results into account (37.8 ± 8.8 % decrease following UVA treatment) (Fig. 3C).

3.2. Experimentally depleting endogenous APP levels ablates UVA-associated reductions in ARPE-19 cell viability

Given the observed decrease in APP and sAPP β levels in ARPE-19 cell cultures following UVA exposure, we wanted to determine whether the protein played any role in UVA-induced

reductions in viable cell numbers. To this end, cells were treated with APP siRNA (see Materials and Methods section) in order to deplete endogenous APP before exposing them to UVA. When cell lysates were prepared and immunoblotted with the anti-APP C-terminal antibody, the results (Fig. 4A) showed a 32.6 ± 2.9 % decrease in full-length APP levels in mock-irradiated cells following APP siRNA treatment (relative to mock-irradiated scramble siRNA cells). Furthermore, APP levels were also decreased following UVA exposure (in the absence of APP siRNA) as previously observed (Fig. 3). These two effects seemed additive in terms of the decreased levels of APP in APP siRNA plus UVA treated cells (Fig. 4A). The cell viability results from parallel experiments showed no effect of APP depletion in mock-irradiated cells (Fig. 4B; compare columns 1 & 2). A significant (25.4 ± 1.7 %) decrease in viable cell numbers was, again, observed following UVA exposure of scramble siRNA-treated cells (compare columns 1 & 3). However, the prior siRNA-mediated depletion of APP was able to protect irradiated cells completely from the effects of UVA (compare columns 3 and 4) restoring viable cell numbers to a level that was no longer significantly different to that of the mock-irradiated controls (94.2 ± 3.1 %).

3.3. α -Secretase inhibition does not modify the effect of UVA on ARPE-19 cell viability

Having established that cellular APP levels are linked to UVA irradiation and that depleting endogenous levels of the protein can modify the effect of UVA irradiation on ARPE-19 cells, we next sought to determine which secretase-mediated events in APP processing, if any, were linked to cellular resistance to UVA irradiation. In order to determine the effect of inhibiting α -secretase APP processing we employed the broad-spectrum matrix metalloproteinase / ADAM inhibitor batimastat ($5 \mu\text{M}$) which caused a 27.2 ± 9.7 % accumulation of full-length APP in cell lysates (Fig. 5A) indicative of strong α -secretase inhibition. Furthermore, sAPP α

production by ARPE-19 cells was reduced by 72.7 ± 6.0 % following batimastat treatment (Fig. 5B) and sAPP β production was not affected (Fig. 5C).

We next pre-treated 80% confluent cells for 6 h with batimastat (5 μ M) before UVA irradiating them and further incubating them in the absence/presence of batimastat for an 18 h recovery period before assessing viable cell numbers. The results (Fig. 5D) show that, in the mock-irradiated cultures, batimastat had no effect on viable cell numbers over the short time course employed. Furthermore, batimastat treatment did not modify the effects of UVA on viable cell numbers (Fig. 5D) suggesting that α -secretase-mediated APP processing does not mediate cellular resistance to UVA irradiation.

3.4. γ -Secretase but not β -secretase inhibition improves ARPE-19 cell resistance to UVA

Having determined that inhibiting non-amyloidogenic APP processing did not modify the effect of UVA on ARPE-19 cell viability we next sought to determine the effects of inhibiting the β - and γ -secretase steps of amyloidogenic processing. Essentially, the experiments described in the preceding section were repeated but using β -secretase inhibitor IV and the notch sparing γ -secretase inhibitor begacestat (GSI-953) (see Materials and Methods section).

We initially determined the effects of β -secretase inhibitor IV on APP processing in ARPE-19 cells using a concentration range of 0-100 nM. The results (Fig. 6A) showed no significant accumulation of full-length APP in cell lysates indicative of amyloidogenic processing being a minor pathway in this cell line. Immunoblotting of the corresponding conditioned medium samples revealed no change in sAPP α production following β -secretase inhibition (Fig. 6B) but a dose-dependent inhibition of sAPP β production (27.9 ± 2.7 , 37.3 ± 4.8 , 50.5 ± 6.0 and

67.3 ± 9.3 % reductions following treatment with 12.5, 25, 50 and 100 nM concentrations of the inhibitor, respectively) (Fig. 6C).

We then investigated whether β -secretase inhibition modified cellular resistance to UVA irradiation as described in the previous section but using 50 nM β -secretase inhibitor IV. The results (Fig. 6D) demonstrated that, even in the mock-irradiated cells, the inhibitor caused a 23.5 ± 9.3 % increase in viable cell numbers (compare columns 1 & 2). As observed previously, UVA irradiation decreased cell viability (by 22.4 ± 2.6 %). However, β -secretase inhibitor IV treatment was unable to modify the resistance of ARPE-19 cells to UVA irradiation (compare columns 3 and 4).

Having ascertained that inhibition of the β -secretase step in amyloidogenic APP processing did not modify cellular resistance to UVA irradiation we next repeated the same experiments using the γ -secretase inhibitor begacestat. This compound has previously been shown to have an IC₅₀ of 12.4 nM in relation to A β 42 generation in SH-SY5Y neuroblastoma cells whilst the same study demonstrated an IC₅₀ in relation to Notch γ -secretase cleavage of 208.5 nM⁴⁴.

We initially determined the effects of begacestat on APP processing in ARPE-19 cells using a concentration range of 0-100 nM. The results showed no significant accumulation of full-length APP in cell lysates (Fig. 7A) but a dose-dependent increase in the levels of APP-CTFs (increases of 57.5 ± 23.5, 132.6 ± 36.5, 182.6 ± 68.3 and 232.4 ± 20.2 % in the presence of 12.5, 25, 50 and 100 nM concentrations of the inhibitor, respectively) (Fig. 7B). This latter result was expected given that γ -secretase cleavage of APP-CTFs should have been inhibited by begacestat. Immunoblotting of the corresponding conditioned medium samples revealed no significant changes in sAPP α and sAPP β generation following γ -secretase inhibition (Figs. 7C and 7D).

We then investigated whether γ -secretase inhibition modified cellular resistance to UVA irradiation using two different begacestat concentrations (25 and 100 nM). The results (Fig. 7E) demonstrated that the inhibitor had no effect on viable cell numbers in mock-irradiated cells (compare column 1 with 2 and 3). Again, UVA irradiation decreased cell viability to 71.3 +/- 1.3 % that of the mock-irradiated cultures (compare columns 1 & 4). Begacestat (100 nM) partly ablated the effect of UVA restoring viable cell numbers to 85.2 \pm 3.2 % those of the mock-irradiated cultures (compare columns 1 and 6). However, this effect was no longer evident at the lower (25 nM) inhibitor concentration.

Collectively, these data demonstrate that, unexpectedly, γ -secretase but not β -secretase inhibition partly ablates the detrimental effect of UVA on ARPE-19 cell viability.

3.5. The effects of secretase-mediated APP proteolysis on long-term culture growth are distinct from those observed in relation to UVA resistance

It was apparent from the effects of UVA exposure on APP levels/proteolysis in ARPE-19 cells (Fig. 3) and our siRNA experiments (Fig. 4) that there is a link between APP and UVA resistance in these cells. Furthermore, it was possible that γ -secretase but not α - or β -secretase APP processing might be responsible for the detrimental effect of APP on viable cell numbers following UVA exposure. However, all of these experiments were performed on 70/80% confluent cell cultures over an approximate 24 h period during which the secretase inhibitors had little to no effect on viable cell counts in the absence of UVA exposure. Given that sAPP α , in particular, has previously been linked to the proliferation of several cell types⁴⁵, we sought to determine whether the effects of secretase-mediated APP processing on the long-term proliferation of ARPE-19 cultures were distinct from those in relation to UVA resistance. To this end, we initially investigated the effects of α -, β - and γ -secretase inhibitors, added at the point of seeding, on viable cell numbers after a seven day growth

period. The α -secretase inhibitor batimastat (5 μ M) reduced viable cell numbers after seven days of growth by 49.2 ± 18.6 % (Fig. 8A) despite not affecting UVA resistance of ARPE-19 cells (Fig. 5D). Cells treated with β -secretase inhibitor IV exhibited no such decrease in viable cell numbers at any of the concentrations employed (Fig. 8B) similar to the lack of effect of this compound in relation to UVA resistance (Fig. 6D). However, the γ -secretase inhibitor begacestat (Fig. 8C) resulted in dose dependant decreases in viable cell numbers of 7.4 ± 2.9 , 13.0 ± 6.2 and 22.1 ± 3.1 % at 25, 50 and 100 nM inhibitor concentrations, respectively (an effect that was seemingly opposite to that observed in relation to UVA resistance; Fig. 7E).

Given the fact that α -secretase inhibition seemed to impair longer-term growth of ARPE-19 cells (and the fact that batimastat is a broad spectrum inhibitor) it was necessary to confirm that the non-amyloidogenic APP fragment, sAPP α , was capable of stimulating growth in this particular cell line. To this end, we co-cultured ARPE-19 cells with HEK cells stably transfected with empty vector (mock transfectants) or plasmids encoding sAPP α or sAPP β (see Materials and Methods). Full-length APP levels in the HEK cells transfected with the two soluble APP constructs were unchanged (Fig. 9A) but the expected sAPP α and sAPP β fragments were clearly highly expressed in their cognate transfectants as shown by their immunodetection in conditioned medium (Figs. 9B and 9C, respectively). In fact, at the levels of immunoblot exposures shown, sAPP α and sAPP β were undetectable other than in medium from their respective transfected cell lines.

Having confirmed the expected over-expression of sAPP α and sAPP β in the HEK stable transfectants, these cells were seeded into ThinCertTM culture inserts and ARPE-19 cells were seeded into the basal wells of the system as described in the Methods section (Fig. 10A).

After seven days, viable ARPE-19 cells in the basal wells were counted (see Materials and

Methods section). The results (Fig. 10B) demonstrated that culturing ARPE-19 cells in the presence of sAPP α -transfected HEK cells led to a 55 ± 12.0 % increase in viable cell numbers relative to cells cultured in the presence of mock-transfected HEK cells. However, no increase in ARPE-19 cell numbers was observed in the presence of sAPP β -transfected HEK cells.

Collectively, these data indicate that α - and possibly γ - but not β -secretase processing of APP impact on long-term ARPE-19 cell proliferation but that these effects are distinct from those observed in relation to the effects of these proteolytic events on the UVA resistance of the same cells.

4. DISCUSSION

Although the evidence is still controversial¹⁶ UV irradiation is considered a possible risk factor in the development of AMD¹³⁻¹⁵. Specifically, short wavelength radiation (UVA radiation of 315-400 nm) is able to penetrate the eye protective structures into the retina¹⁷ inducing significant oxidative stress in the RPE and leading to the formation of, inter alia, drusen deposits¹⁸. These structures contain A β -peptides²²⁻²⁴ that have been associated with key stages in AMD progression and linked to disease aetiology²⁵⁻²⁷. Whilst much literature exists on the potential role of A β -peptides in AMD^{19,21} there is a relative dearth of information on the role of APP in the disease. Therefore, in the current study, we examined the potential role of APP and its proteolytic processing in both the UV resistance and long-term proliferation of human retinal pigment epithelial ARPE-19 cells.

We initially demonstrated that UVA exposure decreases levels of full-length APP in ARPE-19 cells. Whilst this is the first demonstration of this phenomenon in RPE cells, similar results have been observed in a range of other cell lines albeit following UVC or unspecified

UV irradiation^{43, 46, 47} and differentially attributed to reductions in protein levels due to reduced *APP* gene transcription or enhanced secretase-mediated processing of the holoprotein. Notably, when our results were corrected for observed reductions in viable cell numbers following UVA irradiation (which is more reflective of the amount of the fragment generated per cell), we saw no overall change in sAPP α generation which would argue against an up-regulation of non-amyloidogenic processing. Furthermore, the amyloidogenic product, sAPP β , was actually reduced following UV-irradiation. Thus, at least in ARPE-19 cells, it is perhaps more likely that changes in APP levels are the consequence of transcriptional or translational decreases. In this respect it is notable that enhancing levels of the tumour suppressor p53 through various approaches (but not UV irradiation) has previously been shown to repress *APP* promoter activity and subsequent protein expression⁴⁷. In the current study, rather unexpectedly, we did not see an increase in p53 levels in ARPE-19 cells following the 18 h post-irradiation recovery period (data not shown) but this does not preclude an impact of this tumour suppressor on APP expression earlier in the time course.

One of the key findings in the current study is that experimentally depleting APP levels using siRNA completely ablated the detrimental effects of UVA irradiation on ARPE-19 viable cell numbers. This observation indicates that APP has a negative impact on cell survival following UVA irradiation such that its depletion enhances survival which, *prima facie*, seems at odds with the wealth of literature pertaining to the role of APP and sAPP α in cell survival/proliferation/protection³⁷⁻³⁹. However, notably, it has been shown in olfactory sensory neurons derived from BACE1-knockout mouse models that APP over-expression enhances cell death through the intrinsic apoptotic pathway⁴⁸ suggesting that the holoprotein can mediate cell death irrespective of A β -peptide formation. In the current study, the negative impact of APP on viable cell numbers following UVA irradiation did not appear to be related

to the α -secretase-mediated generation of sAPP α as demonstrated by the lack of ability of batimastat to counter the effects of irradiation in this respect. Similarly, despite 50 nM β -secretase inhibitor IV causing an approximately 50% decrease in sAPP β generation, the same concentration of inhibitor did not impact on the decreases in ARPE-19 viable cell numbers observed following UVA irradiation. In contrast, the notch-sparing γ -secretase inhibitor begacestat, at a concentration of 100 nM, did partly ablate the effect of UVA on cell viability. This finding needs to be interpreted with caution as the IC₅₀ value of the inhibitor relative to Notch cleavage has previously been determined to be 208.5 nM⁴⁴; whilst the highest concentration of begacestat employed in the current study was 100 nM it is still possible that some Notch signalling could have been inhibited at this concentration. Notch 2 is the most highly expressed Notch family receptor in ARPE-19 cells and its expression and transcriptional activity of the Notch 2 pathway are enhanced following UVB treatment; an effect which reduces ROS generation and improves cell viability⁴⁹. Similarly, the authors demonstrated that experimental depletion of Notch 2 (using short hairpin RNA) ablated UVB-induced reductions in cell viability but did not employ γ -secretase inhibitors as in the current study. Although the IC₅₀ for begacestat relative, specifically, to Notch 2 has not been reported, a 100 nM concentration of the inhibitor has been shown to reduce Notch transcriptional activity per se by approximately 40% in SH-SY5Y neuroblastoma cells⁴⁴. Furthermore, in the current study, whilst a lower begacestat concentration (25 nM) still caused a 132.6 ± 36.5 % increase in the level of cell-associated APP-CTFs (a direct measure of the inhibition of cleavage of these fragments by γ -secretase), notably, the same inhibitor concentration did not ablate the effects of UVA on ARPE-19 cell viability. The fact that the inhibition of β -secretase in the current study did not affect ARPE-19 resistance to UVA also raises the question as to how, assuming the canonical APP amyloidogenic processing pathway, subsequent γ -secretase inhibition might then improve resistance in this respect.

However, it should be noted that enzymes other than BACE1 (such as Meprin- β ⁵⁰) are able to generate APP-CTFs that are effective γ -secretase substrates (although the involvement of ADAM-generated CTFs would seem to be precluded in the current study by the lack of effect of batimastat on ARPE-19 UVA resistance). Therefore, whilst γ -secretase inhibition clearly enhanced cellular resistance to UVA irradiation in the current study, more work is required in order to unequivocally determine whether this was the consequence of impaired APP processing. However, the combined facts that sAPP β generation was depleted following UVA irradiation and that β -secretase inhibition did not affect ARPE-19 resistance to UVA do serve to indicate that enhanced generation of A β -peptides is not, mechanistically, linked to the fact that APP sensitizes these cells to UVA irradiation.

Whilst full-length APP clearly has a role to play in mediating the ARPE-19 cellular response to UVA irradiation, with the possible exception of γ -secretase, proteolysis of the protein did not appear to be a prerequisite for this functionality. This was somewhat of a surprise given the previously reported beneficial roles of sAPP α in relation to the maintenance of cell viability⁴⁵. As such, we sought to examine the role of APP proteolysis in the longer-term growth of ARPE-19 cells initially by culturing them in the presence of secretase inhibitors. Our results indicate that the amyloidogenic processing of APP plays little role in this respect; β -secretase inhibitor IV barely affected viable cell numbers after seven days of growth and, whilst begacestat did reduce viable cell numbers, as with the UVA experiments discussed above, this only occurred at higher inhibitor concentrations that might impact on Notch signalling and not at the lower concentrations that still inhibited γ -secretase APP-CTF processing. In contrast, inhibition of α -secretase-mediated APP processing using batimastat (5 μ M) clearly impaired proliferation of ARPE-19 cells over seven days. The batimastat dose in the current study was selected to give effective α -secretase inhibition based on our

previous finding⁵¹ that the batimastat IC₅₀ for α -secretase is 1.2 μ M in cell-based experiments (note that none of the inhibitors employed exhibited any cytotoxicity at the concentrations used; data not shown). Nonetheless, batimastat is a broad spectrum inhibitor and, therefore, whilst these initial experiments indicated that sAPP α plays a role in ARPE-19 cell proliferation, it was necessary to confirm this through an alternative experimental approach. In this respect, our ARPE-19/HEK co-culture results further underpin a role for sAPP α but not sAPP β in the proliferation of the former cell line. These results are consistent with previous findings in other cell lines demonstrating a role for sAPP α in cell proliferation that seems dependent on the C-terminal 16 amino acids of the fragment that are absent in sAPP β ⁵².

CONCLUSION

Collectively, our data demonstrate, for the first time, a role for the APP holoprotein in mediating the effects of UVA irradiation in retinal pigment epithelial cells. This effect is not dependant on canonical secretase-mediated processing of the protein and is, therefore, distinct from the beneficial role played by sAPP α in the proliferation of the same cell type. Whilst these effects are clearly differential, our results indicate that APP should be investigated further in relation to the identification of possible drug targets for the treatment of AMD.

ETHICS APPROVAL AND CONSENT TO PARTICIPATE

Not applicable

HUMAN AND ANIMAL RIGHTS

No animals/humans were used for the studies in this research.

CONSENT FOR PUBLICATION

Not applicable

CONFLICT OF INTEREST

The authors declare no conflict of interest, financial or otherwise.

REFERENCES

1. Klein, R.; Klein, B. E.; Knudtson, M. D.; Meuer, S. M.; Swift, M.; Gangnon, R. E., Fifteen-year cumulative incidence of age-related macular degeneration: the Beaver Dam Eye Study. *Ophthalmology* **2007**, *114* (2), 253-62.
2. Wong, W. L.; Su, X.; Li, X.; Cheung, C. M. G.; Klein, R.; Cheng, C.-Y.; Wong, T. Y., Global prevalence of age-related macular degeneration and disease burden projection for 2020 and 2040: a systematic review and meta-analysis. *The Lancet Global Health* **2014**, *2* (2), e106-e116.
3. Salvi, S. M.; Akhtar, S.; Currie, Z., Ageing changes in the eye. *Postgrad Med J* **2006**, *82* (971), 581-587.
4. Mathenge, W., Age-related macular degeneration. *Community Eye Health* **2014**, *27* (87), 49-50.
5. Parment, S.; Lynn, C.; Glass, R. M., Age-Related Macular Degeneration. *JAMA* **2006**, *295* (20), 2438-2438.
6. Hernández-Zimbrón, L. F.; Zamora-Alvarado, R.; Ochoa-De la Paz, L.; Velez-Montoya, R.; Zenteno, E.; Gullías-Cañizo, R.; Quiroz-Mercado, H.; Gonzalez-Salinas, R., Age-Related Macular Degeneration: New Paradigms for Treatment and Management of AMD. *Oxid Med Cell Longev* **2018**, *2018*, 8374647-8374647.
7. Chalam, K. V.; Khetpal, V.; Rusovici, R.; Balaiya, S., A review: role of ultraviolet radiation in age-related macular degeneration. *Eye Contact Lens* **2011**, *37* (4), 225-32.
8. McCubrey, J. A.; Lahair, M. M.; Franklin, R. A., Reactive oxygen species-induced activation of the MAP kinase signaling pathways. *Antioxidants & redox signaling* **2006**, *8* (9-10), 1775-89.
9. Patton, W. P.; Chakravarthy, U.; Davies, R. J.; Archer, D. B., Comet assay of UV-induced DNA damage in retinal pigment epithelial cells. *Invest Ophthalmol Vis Sci* **1999**, *40* (13), 3268-75.
10. Roduit, R.; Schorderet, D. F., MAP kinase pathways in UV-induced apoptosis of retinal pigment epithelium ARPE19 cells. *Apoptosis : an international journal on programmed cell death* **2008**, *13* (3), 343-53.

11. Sheu, S. J.; Wu, S. N., Mechanism of inhibitory actions of oxidizing agents on calcium-activated potassium current in cultured pigment epithelial cells of the human retina. *Invest Ophthalmol Vis Sci* **2003**, *44* (3), 1237-44.
12. Tratsk, K. S.; Thanos, S., UV irradiation causes multiple cellular changes in cultured human retinal pigment epithelium cells. *Graefe's archive for clinical and experimental ophthalmology = Albrecht von Graefes Archiv fur klinische und experimentelle Ophthalmologie* **2003**, *241* (10), 852-9.
13. Fletcher, A. E.; Bentham, G. C.; Agnew, M.; Young, I. S.; Augood, C.; Chakravarthy, U.; de Jong, P. T.; Rahu, M.; Seland, J.; Soubrane, G.; Tomazzoli, L.; Topouzis, F.; Vingerling, J. R.; Vioque, J., Sunlight exposure, antioxidants, and age-related macular degeneration. *Arch Ophthalmol* **2008**, *126* (10), 1396-403.
14. Vojniković, B.; Njirić, S.; Čoklo, M.; Spanjol, J., Ultraviolet sun radiation and incidence of age-related macular degeneration on Croatian Island Rab. *Collegium antropologicum* **2007**, *31 Suppl 1*, 43-4.
15. Plestina-Borjan, I.; Klinger-Lasić, M., Long-term exposure to solar ultraviolet radiation as a risk factor for age-related macular degeneration. *Collegium antropologicum* **2007**, *31 Suppl 1*, 33-8.
16. Zhou, H.; Zhang, H.; Yu, A.; Xie, J., Association between sunlight exposure and risk of age-related macular degeneration: a meta-analysis. *BMC Ophthalmology* **2018**, *18* (1), 331.
17. Glickman, R. D., Ultraviolet phototoxicity to the retina. *Eye Contact Lens* **2011**, *37* (4), 196-205.
18. Nowak, M.; Gnitecki, W.; Jurowski, P., [The role of retinal oxygen metabolism in origin of age-related macular degeneration (AMD)]. *Klin Oczna* **2005**, *107* (10-12), 715-8.
19. Ashok, A.; Singh, N.; Chaudhary, S.; Bellamkonda, V.; Kritikos, A. E.; Wise, A. S.; Rana, N.; McDonald, D.; Ayyagari, R., Retinal Degeneration and Alzheimer's Disease: An Evolving Link. *International journal of molecular sciences* **2020**, *21* (19).
20. Wang, L.; Mao, X., Role of Retinal Amyloid-beta in Neurodegenerative Diseases: Overlapping Mechanisms and Emerging Clinical Applications. *International journal of molecular sciences* **2021**, *22* (5).
21. Zhao, Y.; Bhattacharjee, S.; Jones, B. M.; Hill, J. M.; Clement, C.; Sambamurti, K.; Dua, P.; Lukiw, W. J., Beta-Amyloid Precursor Protein (betaAPP) Processing in Alzheimer's Disease (AD) and Age-Related Macular Degeneration (AMD). *Molecular neurobiology* **2015**, *52* (1), 533-44.
22. Anderson, D. H.; Talaga, K. C.; Rivest, A. J.; Barron, E.; Hageman, G. S.; Johnson, L. V., Characterization of beta amyloid assemblies in drusen: the deposits associated with aging and age-related macular degeneration. *Exp Eye Res* **2004**, *78* (2), 243-56.
23. Luibl, V.; Isas, J. M.; Kaye, R.; Glabe, C. G.; Langen, R.; Chen, J., Drusen deposits associated with aging and age-related macular degeneration contain nonfibrillar amyloid oligomers. *The Journal of clinical investigation* **2006**, *116* (2), 378-385.
24. Dentchev, T.; Milam, A. H.; Lee, V. M.; Trojanowski, J. Q.; Dunaief, J. L., Amyloid-beta is found in drusen from some age-related macular degeneration retinas, but not in drusen from normal retinas. *Mol Vis* **2003**, *9*, 184-90.
25. Ratnayaka, J. A.; Serpell, L. C.; Lotery, A. J., Dementia of the eye: the role of amyloid beta in retinal degeneration. *Eye* **2015**, *29* (8), 1013-1026.
26. Ohno-Matsui, K., Parallel findings in age-related macular degeneration and Alzheimer's disease. *Prog Retin Eye Res* **2011**, *30* (4), 217-38.
27. Johnson, L. V.; Leitner, W. P.; Rivest, A. J.; Staples, M. K.; Radeke, M. J.; Anderson, D. H., The Alzheimer's A beta -peptide is deposited at sites of complement activation in pathologic deposits associated with aging and age-related macular degeneration. *Proceedings of the National Academy of Sciences of the United States of America* **2002**, *99* (18), 11830-11835.
28. Prasad, T.; Zhu, P.; Verma, A.; Chakrabarty, P.; Rosario, A. M.; Golde, T. E.; Li, Q., Amyloid β peptides overexpression in retinal pigment epithelial cells via AAV-mediated gene transfer mimics AMD-like pathology in mice. *Sci Rep* **2017**, *7* (1), 3222.

29. Dawson, D. W.; Volpert, O. V.; Gillis, P.; Crawford, S. E.; Xu, H.; Benedict, W.; Bouck, N. P., Pigment epithelium-derived factor: a potent inhibitor of angiogenesis. *Science* **1999**, *285* (5425), 245-8.
30. Yoshida, T.; Ohno-Matsui, K.; Ichinose, S.; Sato, T.; Iwata, N.; Saido, T. C.; Hisatomi, T.; Mochizuki, M.; Morita, I., The potential role of amyloid beta in the pathogenesis of age-related macular degeneration. *The Journal of clinical investigation* **2005**, *115* (10), 2793-2800.
31. Koyama, Y.; Matsuzaki, S.; Gomi, F.; Yamada, K.; Katayama, T.; Sato, K.; Kumada, T.; Fukuda, A.; Matsuda, S.; Tano, Y.; Tohyama, M., Induction of Amyloid β Accumulation by ER Calcium Disruption and Resultant Upregulation of Angiogenic Factors in ARPE19 Cells. *Investigative Ophthalmology & Visual Science* **2008**, *49* (6), 2376-2383.
32. Andrew, R. J.; Kellett, K. A.; Thinakaran, G.; Hooper, N. M., A Greek Tragedy: The Growing Complexity of Alzheimer Amyloid Precursor Protein Proteolysis. *J Biol Chem* **2016**, *291* (37), 19235-44.
33. Yuksel, M.; Tacal, O., Trafficking and proteolytic processing of amyloid precursor protein and secretases in Alzheimer's disease development: An up-to-date review. *European journal of pharmacology* **2019**, *856*, 172415.
34. Postina, R.; Schroeder, A.; Dewachter, I.; Bohl, J.; Schmitt, U.; Kojro, E.; Prinzen, C.; Endres, K.; Hiemke, C.; Blessing, M.; Flamez, P.; Dequenue, A.; Godaux, E.; van Leuven, F.; Fahrenholz, F., A disintegrin-metalloproteinase prevents amyloid plaque formation and hippocampal defects in an Alzheimer disease mouse model. *J Clin Invest* **2004**, *113* (10), 1456-64.
35. Gough, M.; Parr-Sturgess, C.; Parkin, E., Zinc metalloproteinases and amyloid Beta-Peptide metabolism: the positive side of proteolysis in Alzheimer's disease. *Biochem Res Int* **2011**, *2011*, 721463.
36. Dar, N. J.; Glazner, G. W., Deciphering the neuroprotective and neurogenic potential of soluble amyloid precursor protein alpha (sAPPalpha). *Cellular and molecular life sciences : CMLS* **2020**, *77* (12), 2315-2330.
37. Araki, W.; Kitaguchi, N.; Tokushima, Y.; Ishii, K.; Aratake, H.; Shimohama, S.; Nakamura, S.; Kimura, J., Trophic effect of beta-amyloid precursor protein on cerebral cortical neurons in culture. *Biochem Biophys Res Commun* **1991**, *181* (1), 265-71.
38. Goodman, Y.; Mattson, M. P., Secreted forms of beta-amyloid precursor protein protect hippocampal neurons against amyloid beta-peptide-induced oxidative injury. *Experimental neurology* **1994**, *128* (1), 1-12.
39. Mattson, M. P.; Cheng, B.; Culwell, A. R.; Esch, F. S.; Lieberburg, I.; Rydel, R. E., Evidence for excitoprotective and intraneuronal calcium-regulating roles for secreted forms of the beta-amyloid precursor protein. *Neuron* **1993**, *10* (2), 243-54.
40. Parkin, E. T.; Watt, N. T.; Hussain, I.; Eckman, E. A.; Eckman, C. B.; Manson, J. C.; Baybutt, H. N.; Turner, A. J.; Hooper, N. M., Cellular prion protein regulates beta-secretase cleavage of the Alzheimer's amyloid precursor protein. *Proc Natl Acad Sci U S A* **2007**, *104* (26), 11062-7.
41. Smith, P. K.; Krohn, R. I.; Hermanson, G. T.; Mallia, A. K.; Gartner, F. H.; Provenzano, M. D.; Fujimoto, E. K.; Goeke, N. M.; Olson, B. J.; Klenk, D. C., Measurement of protein using bicinchoninic acid. *Anal Biochem* **1985**, *150* (1), 76-85.
42. Hooper, N. M.; Turner, A. J., Isolation of two differentially glycosylated forms of peptidyl-dipeptidase A (angiotensin converting enzyme) from pig brain: a re-evaluation of their role in neuropeptide metabolism. *Biochem J* **1987**, *241* (3), 625-33.
43. Almenar-Queralt, A.; Falzone, T. L.; Shen, Z.; Lillo, C.; Killian, R. L.; Arreola, A. S.; Niederst, E. D.; Ng, K. S.; Kim, S. N.; Briggs, S. P.; Williams, D. S.; Goldstein, L. S., UV irradiation accelerates amyloid precursor protein (APP) processing and disrupts APP axonal transport. *The Journal of neuroscience : the official journal of the Society for Neuroscience* **2014**, *34* (9), 3320-39.
44. Martone, R. L.; Zhou, H.; Atchison, K.; Comery, T.; Xu, J. Z.; Huang, X.; Gong, X.; Jin, M.; Kreft, A.; Harrison, B.; Mayer, S. C.; Aschmies, S.; Gonzales, C.; Zaleska, M. M.; Riddell, D. R.; Wagner, E.; Lu, P.; Sun, S. C.; Sonnenberg-Reines, J.; Oganessian, A.; Adkins, K.; Leach, M. W.;

- Clarke, D. W.; Hury, D.; Abou-Gharbia, M.; Magolda, R.; Bard, J.; Frick, G.; Raje, S.; Forlow, S. B.; Balliet, C.; Burczynski, M. E.; Reinhart, P. H.; Wan, H. I.; Pangalos, M. N.; Jacobsen, J. S., Begacestat (GSI-953): a novel, selective thiophene sulfonamide inhibitor of amyloid precursor protein gamma-secretase for the treatment of Alzheimer's disease. *J Pharmacol Exp Ther* **2009**, *331* (2), 598-608.
45. Corbett, N. J.; Hooper, N. M., Soluble Amyloid Precursor Protein alpha: Friend or Foe? *Adv Exp Med Biol* **2018**, *1112*, 177-183.
46. Cuesta, A.; Zambrano, A.; Lopez, E.; Pascual, A., Thyroid hormones reverse the UV-induced repression of APP in neuroblastoma cells. *FEBS letters* **2009**, *583* (14), 2401-6.
47. Cuesta, A.; Zambrano, A.; Royo, M.; Pascual, A., The tumour suppressor p53 regulates the expression of amyloid precursor protein (APP). *Biochem J* **2009**, *418* (3), 643-50.
48. Cheng, N.; Jiao, S.; Gumaste, A.; Bai, L.; Belluscio, L., APP Overexpression Causes Abeta-Independent Neuronal Death through Intrinsic Apoptosis Pathway. *eNeuro* **2016**, *3* (4).
49. Liu, L.; Zhou, X.; Kuang, X.; Long, C.; Liu, W.; Tang, Y.; Liu, H.; He, J.; Huang, Z.; Fan, Y.; Zhang, Q.; Shen, H., The inhibition of NOTCH2 reduces UVB-induced damage in retinal pigment epithelium cells. *Molecular medicine reports* **2017**, *16* (1), 730-736.
50. Scharfenberg, F.; Armbrust, F.; Marengo, L.; Pietrzik, C.; Becker-Pauly, C., Regulation of the alternative beta-secretase meprin beta by ADAM-mediated shedding. *Cellular and molecular life sciences : CMLS* **2019**, *76* (16), 3193-3206.
51. Parkin, E. T.; Trew, A.; Christie, G.; Faller, A.; Mayer, R.; Turner, A. J.; Hooper, N. M., Structure-activity relationship of hydroxamate-based inhibitors on the secretases that cleave the amyloid precursor protein, angiotensin converting enzyme, CD23, and pro-tumor necrosis factor-alpha. *Biochemistry* **2002**, *41* (15), 4972-81.
52. Chasseigneaux, S.; Allinquant, B., Functions of Abeta, sAPPalpha and sAPPbeta : similarities and differences. *J Neurochem* **2012**, *120 Suppl 1*, 99-108.

FIGURE LEGENDS

Figure 1. Amyloidogenic and non-amyloidogenic processing of the amyloid precursor protein. In the amyloidogenic pathway, full-length amyloid precursor protein (FL-APP) is initially cleaved at the N-terminus of the amyloid beta (A β) region by β -secretase to generate soluble APP β (sAPP β) and a membrane-associated C-terminal fragment, CTF β . The latter product is then further processed by the γ -secretase complex to generate intact A β -peptides and the APP intracellular domain (AICD). Conversely, in the non-amyloidogenic pathway, FL-APP is processed by an α -secretase that cleaves within the A β region forming soluble APP α and a membrane-associated C-terminal fragment (CTF α).

Figure 2. The effect of UVA irradiation on ARPE-19 cell viability. Cells (80% confluent) were irradiated with UVA doses of 0-263 kJm⁻² with an 18 h recovery period before

determination of cell viability as described in the Materials and Methods section. Results are expressed as a percentage of mock-irradiated control cell viability and are means \pm S.D.

(n=3). *****, $p < 0.000001$, compared with the control.

Figure 3. The effect of UVA irradiation on full-length APP, sAPP α and sAPP β in ARPE-19 cells. Cells (80% confluent) were irradiated with UVA (105 kJm⁻²) with an 18 h recovery period as described in the Materials and Methods section. Cell lysates and concentrated conditioned medium samples were then prepared and equal amounts of protein (lysates) or equal sample volumes (medium) were subjected to SDS-PAGE and immunoblotting (see Materials and Methods section). **(A)** Detection of full-length APP (using anti-APP C-terminal antibody) and actin in lysates. **(B)** Detection of sAPP α in medium (using anti-APP 6E10 antibody). **(C)** Detection of sAPP β in medium. Multiple immunoblots were quantified by densitometric analysis and results are expressed as a percentage of mock-irradiated control cell protein levels (means \pm S.D., n=3). For the two medium immunoblots the results before and after correcting for variations in cell viability are shown. *, $p < 0.05$; ***, $p < 0.001$, compared with the control. Dashed lines indicate where lanes from the same representative immunoblot have been rearranged for illustrative purposes.

Figure 4. The effect of experimental APP depletion on UVA-associated reductions in ARPE-19 cell viability. Cells (70% confluent) were treated with scramble or APP siRNA and subsequently irradiated with UVA (105 kJm⁻²) with an 18 h recovery period as described in the Materials and Methods section. Cell viability was determined and cell lysates were then prepared before subjecting equal amounts of protein to SDS-PAGE and immunoblotting (see Materials and Methods section). **(A)** Detection of full-length APP (using anti-APP C-terminal antibody) and actin in lysates. Multiple immunoblots were quantified by densitometric analysis. **(B)** Cell viability. All results are expressed as a percentage of mock-irradiated

scramble siRNA control cell samples (means \pm S.D., n=3). *, $p < 0.05$; **, $p < 0.01$; ***, $p < 0.001$; ****, $p < 0.0001$.

Figure 5. The effect of α -secretase inhibition on APP processing and UVA-associated reductions in ARPE-19 cell viability. **(A-C)** Confluent flasks of cells were treated plus/minus batimastat (5 μ M) for 24 h before harvesting cells and conditioned medium. Equal amounts of protein (lysates) or equal sample volumes (medium) were subjected to SDS-PAGE and immunoblotting (see Materials and Methods section). **(A)** Detection of full-length APP (using anti-APP C-terminal antibody) and actin in lysates. **(B)** Detection of sAPP α in medium (using anti-APP 6E10 antibody). **(C)** Detection of sAPP β in medium. Multiple immunoblots were quantified by densitometric analysis. **(D)** Cells (80% confluent) were irradiated with UVA (105 kJm⁻²) with an 18 h recovery period (all plus/minus batimastat, 5 μ M) before determination of cell viability as described in the Materials and Methods section. Results are expressed as a percentage of untreated control cell samples (means \pm S.D., n=4). *, $p < 0.05$; **, $p < 0.01$; ***, $p < 0.001$.

Figure 6. The effect of β -secretase inhibition on APP processing and UVA-associated reductions in ARPE-19 cell viability. **(A-C)** Confluent flasks of cells were treated plus/minus β -secretase inhibitor IV (0-100 nM) for 24 h before harvesting cells and conditioned medium. Equal amounts of protein (lysates) or equal sample volumes (medium) were subjected to SDS-PAGE and immunoblotting (see Materials and Methods section). **(A)** Detection of full-length APP (using anti-APP C-terminal antibody) and actin in lysates. **(B)** Detection of sAPP α in medium (using anti-APP 6E10 antibody). **(C)** Detection of sAPP β in medium. Multiple immunoblots were quantified by densitometric analysis. **(D)** Cells (80% confluent) were irradiated with UVA (105 kJm⁻²) with an 18 h recovery period (all plus/minus β -secretase inhibitor IV, 50 nM) before determination of cell viability as described in the

Materials and Methods section. Results are expressed as a percentage of untreated control cell samples (means \pm S.D., n=4). *, $p < 0.05$; **, $p < 0.01$; ***, $p < 0.001$; ****, $p < 0.0001$; *****, $p < 0.000001$.

Figure 7. The effect of γ -secretase inhibition on APP processing and UVA-associated reductions in ARPE-19 cell viability. **(A-D)** Confluent flasks of cells were treated plus/minus begacestat (0-100 nM) for 24 h before harvesting cells and conditioned medium. Equal amounts of protein (lysates) or equal sample volumes (medium) were subjected to SDS-PAGE and immunoblotting (see Materials and Methods section). **(A)** Detection of full-length APP (using anti-APP C-terminal antibody) and actin in lysates. **(B)** Detection of APP C-terminal fragments in lysates (using anti-APP C-terminal antibody). **(C)** Detection of sAPP α in medium (using anti-APP 6E10 antibody). **(D)** Detection of sAPP β in medium. Multiple immunoblots were quantified by densitometric analysis. **(E)** Cells (80% confluent) were irradiated with UVA (105 kJm⁻²) with an 18 h recovery period (all plus/minus begacestat, 25 or 100 nM) before determination of cell viability as described in the Materials and Methods section. Results are expressed as a percentage of untreated control cell samples (means \pm S.D., n=4). *, $p < 0.05$; **, $p < 0.01$; *****, $p < 0.00001$; *****, $p < 0.000001$.

Figure 8. The effect of secretase inhibitors on ARPE-19 cell long-term proliferation. Secretase inhibitors (**(A)** batimastat, 5 μ M; **(B)** β -secretase inhibitor IV, 0-100 nM; **(C)** begacestat, 0-100 nM) were added to cultures at the point of seeding. Medium was changed and fresh inhibitor was added every 48 h for seven days at which point viable cell numbers were determined as described in the Materials and Methods section. Results are expressed as a percentage of no inhibitor control viable cell numbers and are means \pm S.D. (n=3). *, $p < 0.05$; **, $p < 0.01$.

Figure 9. Characterisation of HEK cell stable transfectants. Cells were stably transfected with empty vector (mock) or plasmids encoding sAPP α or sAPP β as described in the Materials and Methods section. Confluent flasks of cells were then transferred into UltraMEMTM reduced serum medium for 24 h. Cell lysates and concentrated conditioned medium samples were then prepared and equal amounts of protein (lysates) or equal sample volumes (medium) were subjected to SDS-PAGE and immunoblotting (see Materials and Methods section). **(A)** Detection of full-length APP (using anti-APP C-terminal antibody) and actin in lysates. **(B)** Detection of sAPP α in medium (using anti-APP 6E10 antibody). **(C)** Detection of sAPP β in medium. Multiple immunoblots were quantified by densitometric analysis and the results for full-length APP are expressed as a percentage of the mock-transfected control levels whereas the two soluble APP fragment results are expressed as a percentage of their cognate transfectant as the fragments were not detected in medium from the other transfectants at the immunoblot exposures shown. All results are means \pm S.D. (n=4). Dashed lines indicate where lanes from the same representative immunoblot have been rearranged for illustrative purposes.

Figure 10. The effect of HEK cell stable transfectants on ARPE-19 cell long-term proliferation in co-cultures. HEK cells transfected with empty vector (mock) or plasmids encoding sAPP α or sAPP β were seeded into culture inserts and co-cultured with ARPE-19 cells in the basal wells of the system **(A)** for a seven day period as described in the Materials and Methods section. **(B)** Determination of viable ARPE-19 cell numbers in co-cultures after seven days. Results are expressed as a percentage of ARPE-19 viable cell numbers in the mock-transfected HEK cell control co-cultures and are means \pm S.D. (n=6). ***, $p \leq 0.0001$.

Figure 1

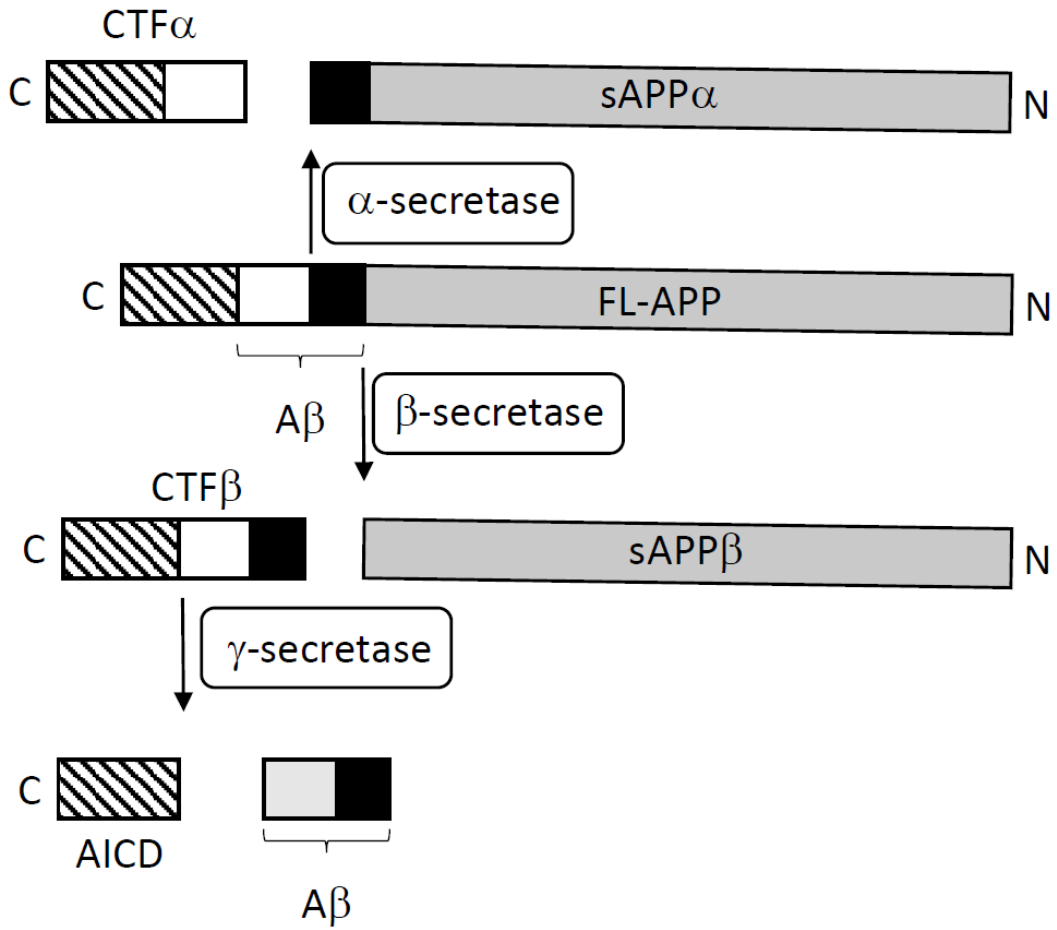


Figure 2

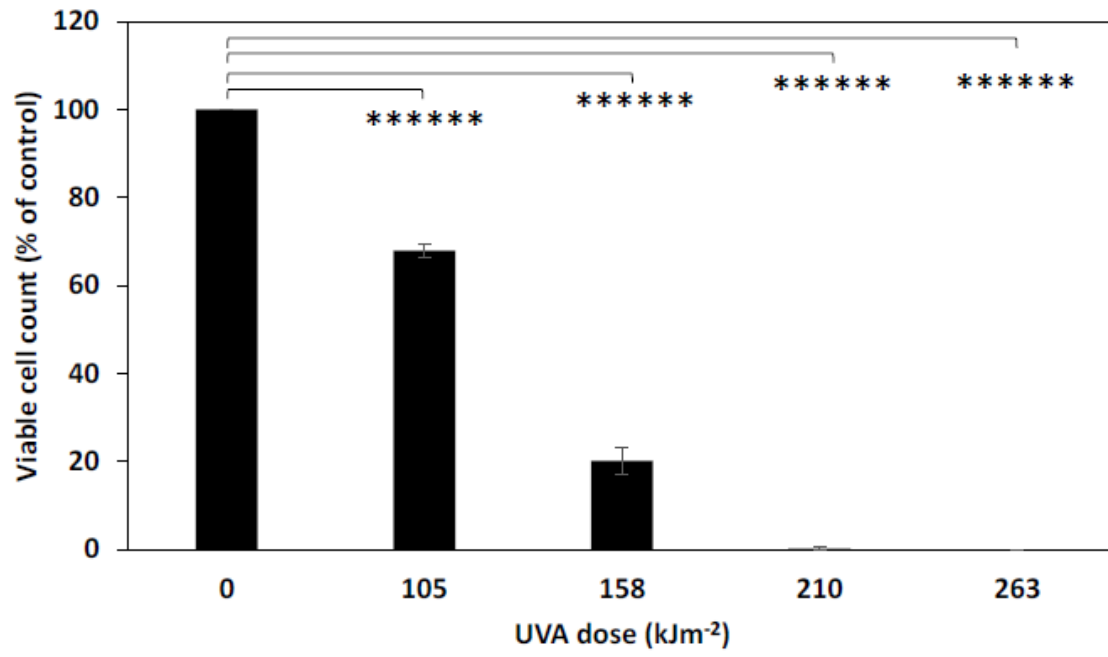


Figure 3

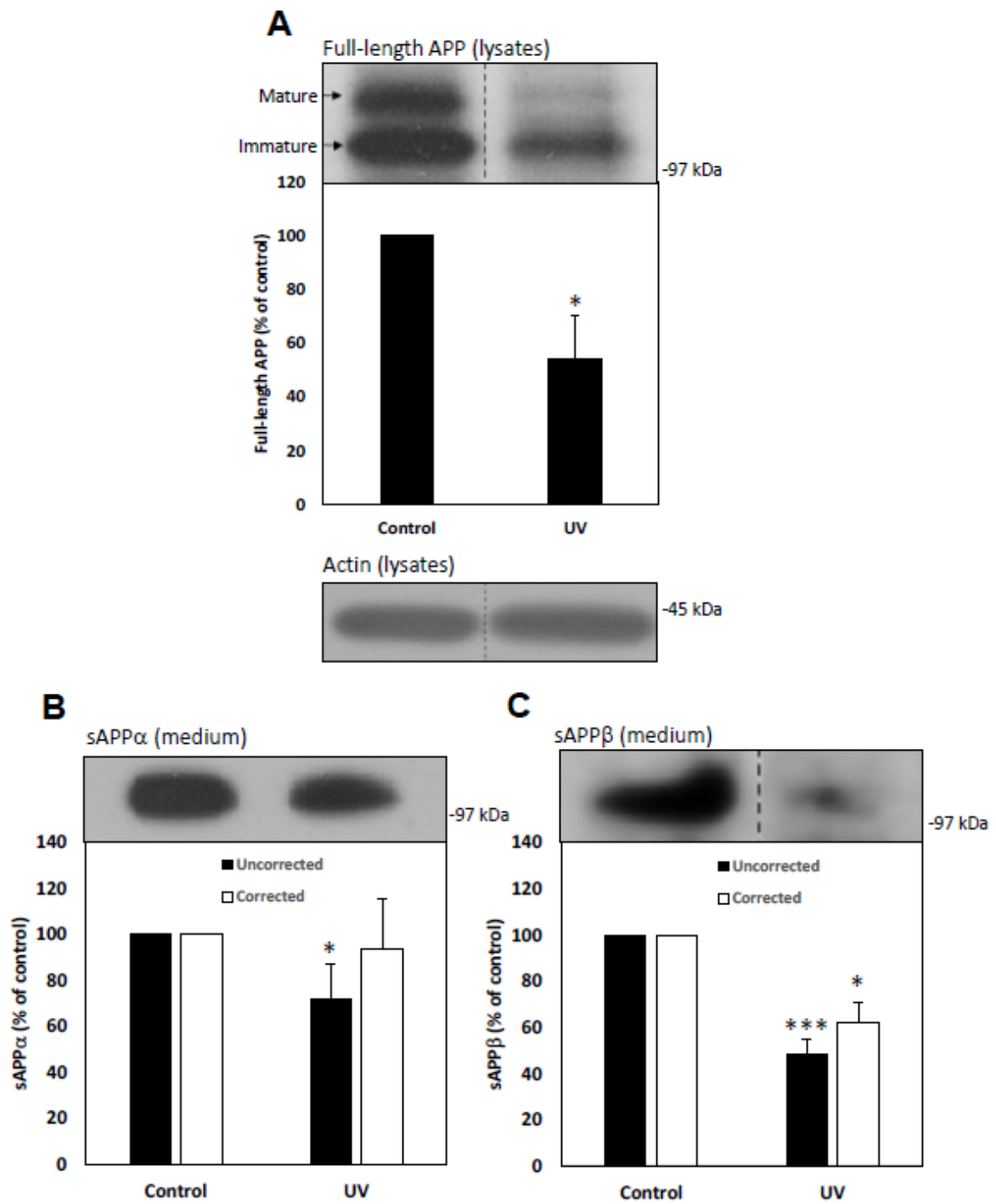


Figure 4

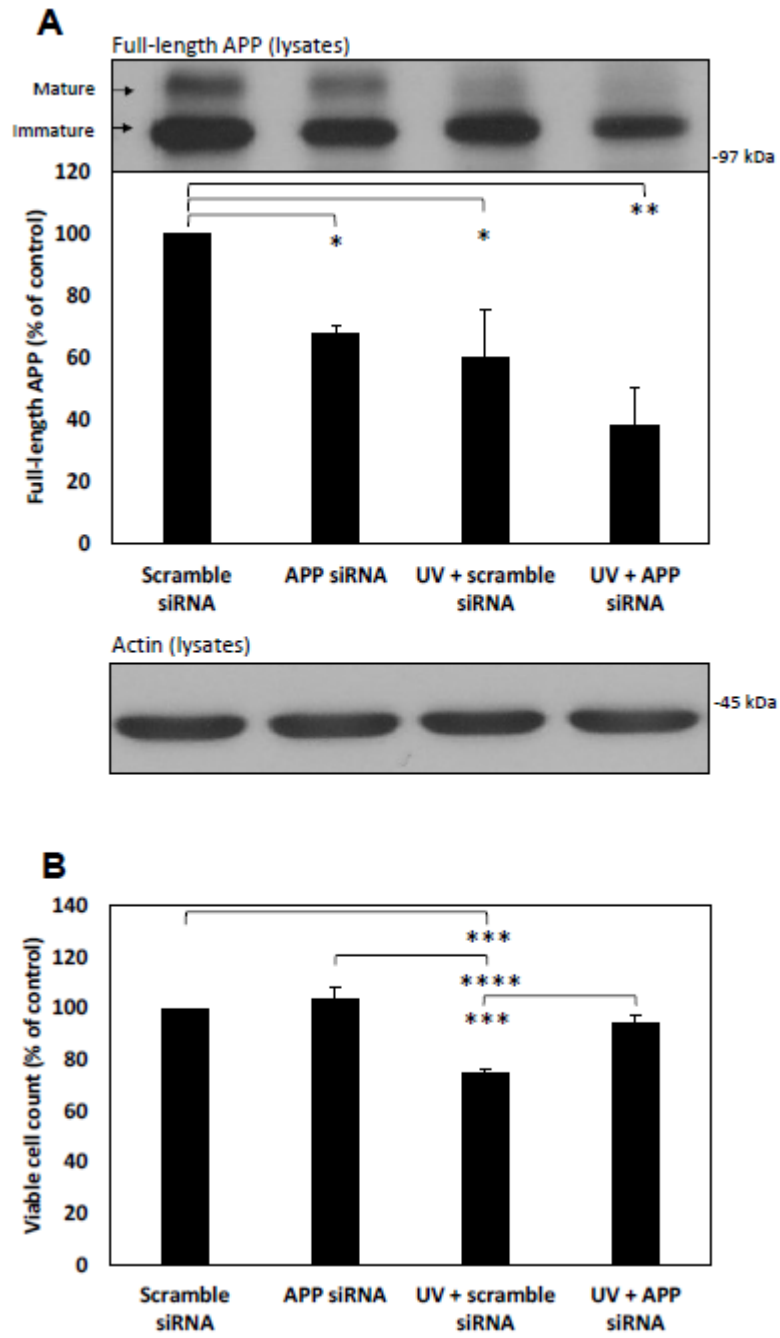


Figure 5

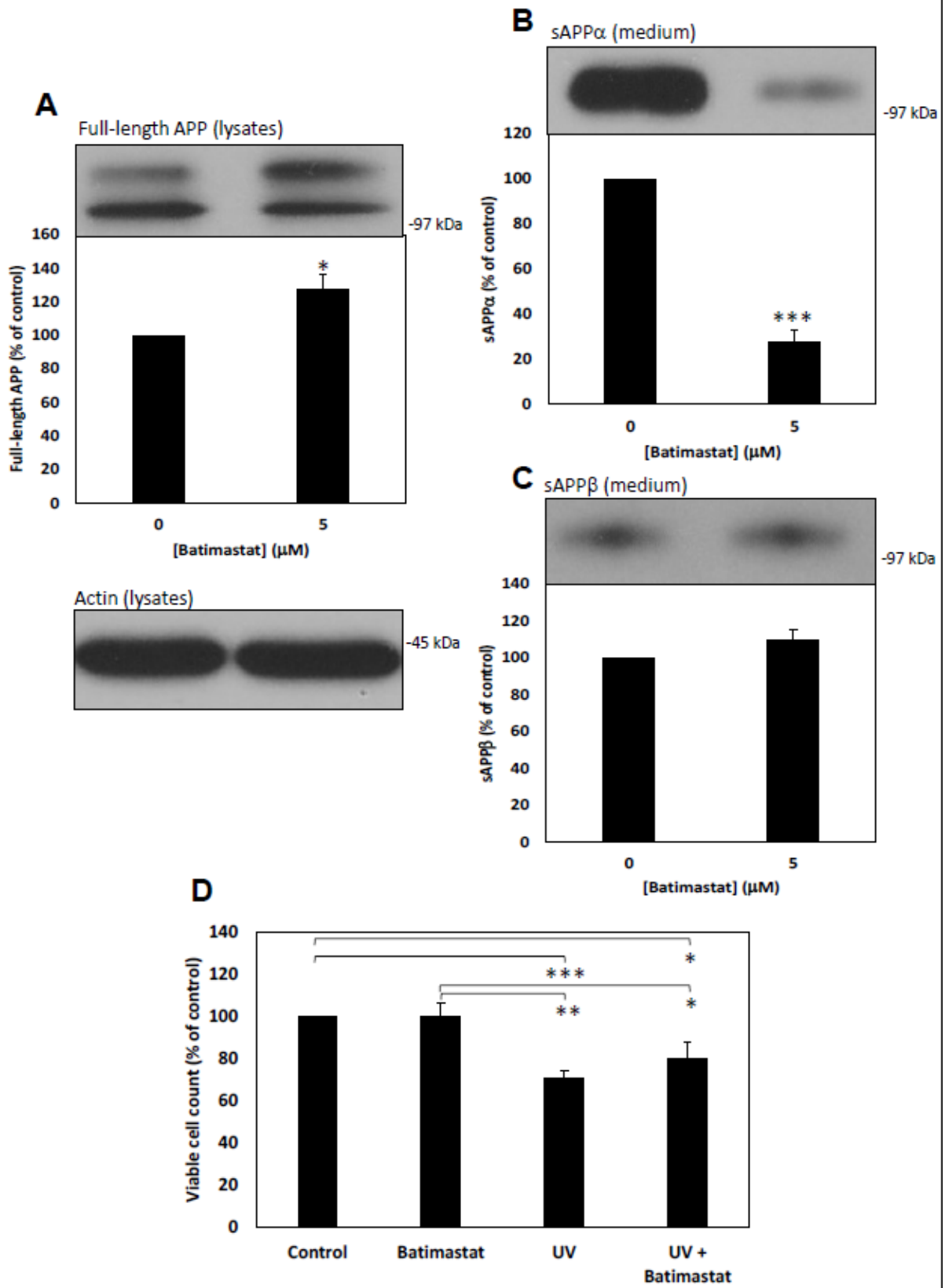


Figure 6

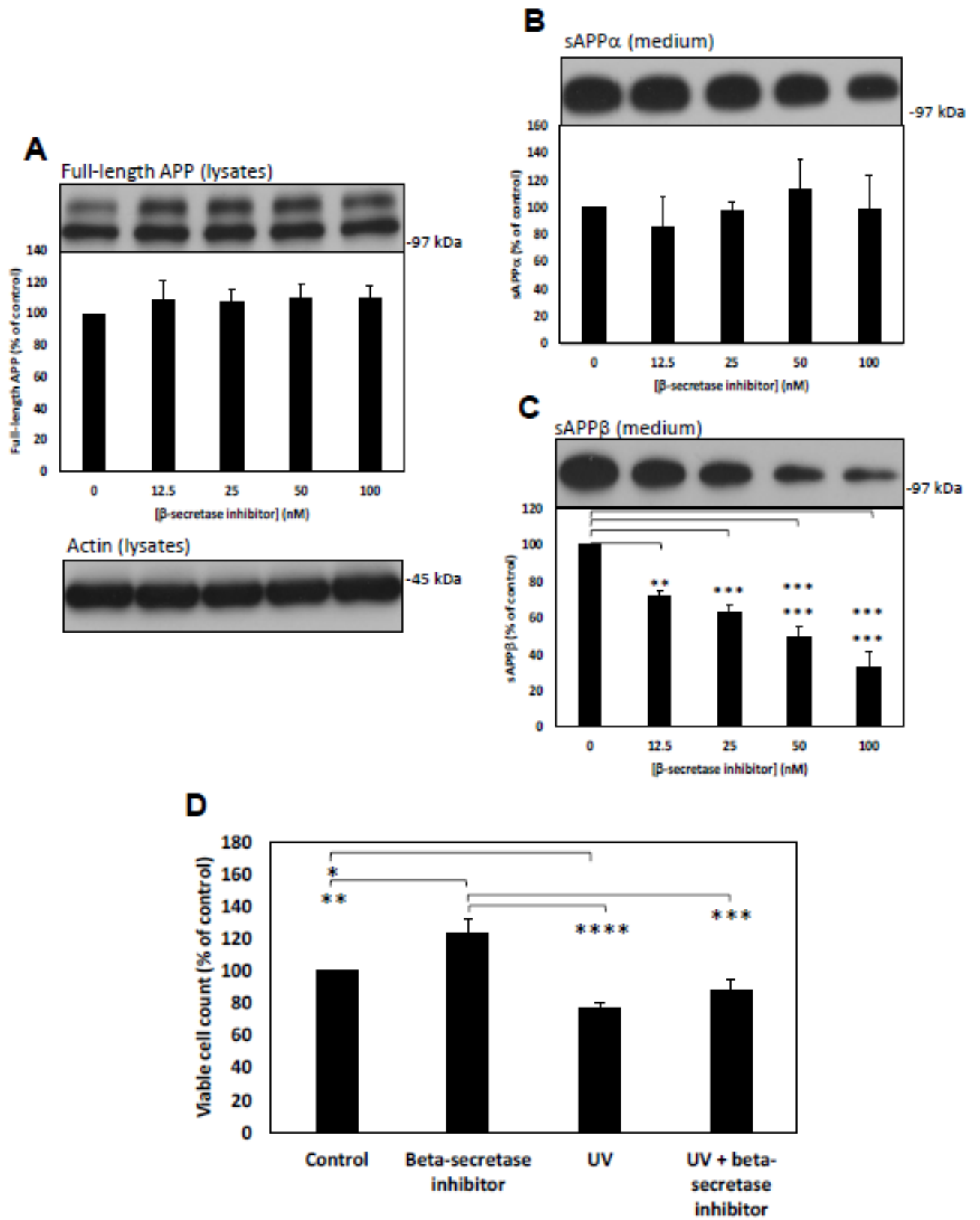


Figure 7

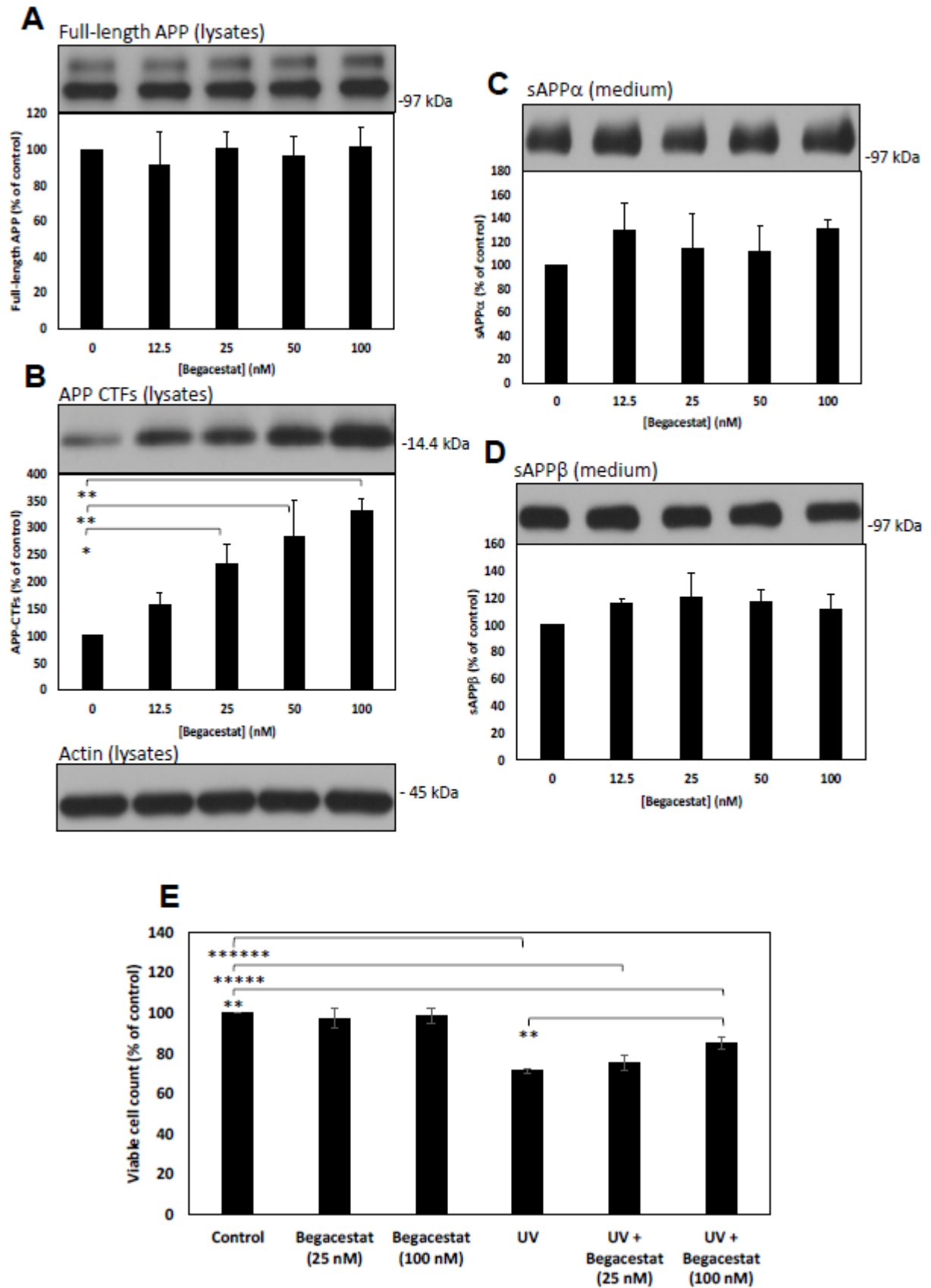


Figure 8

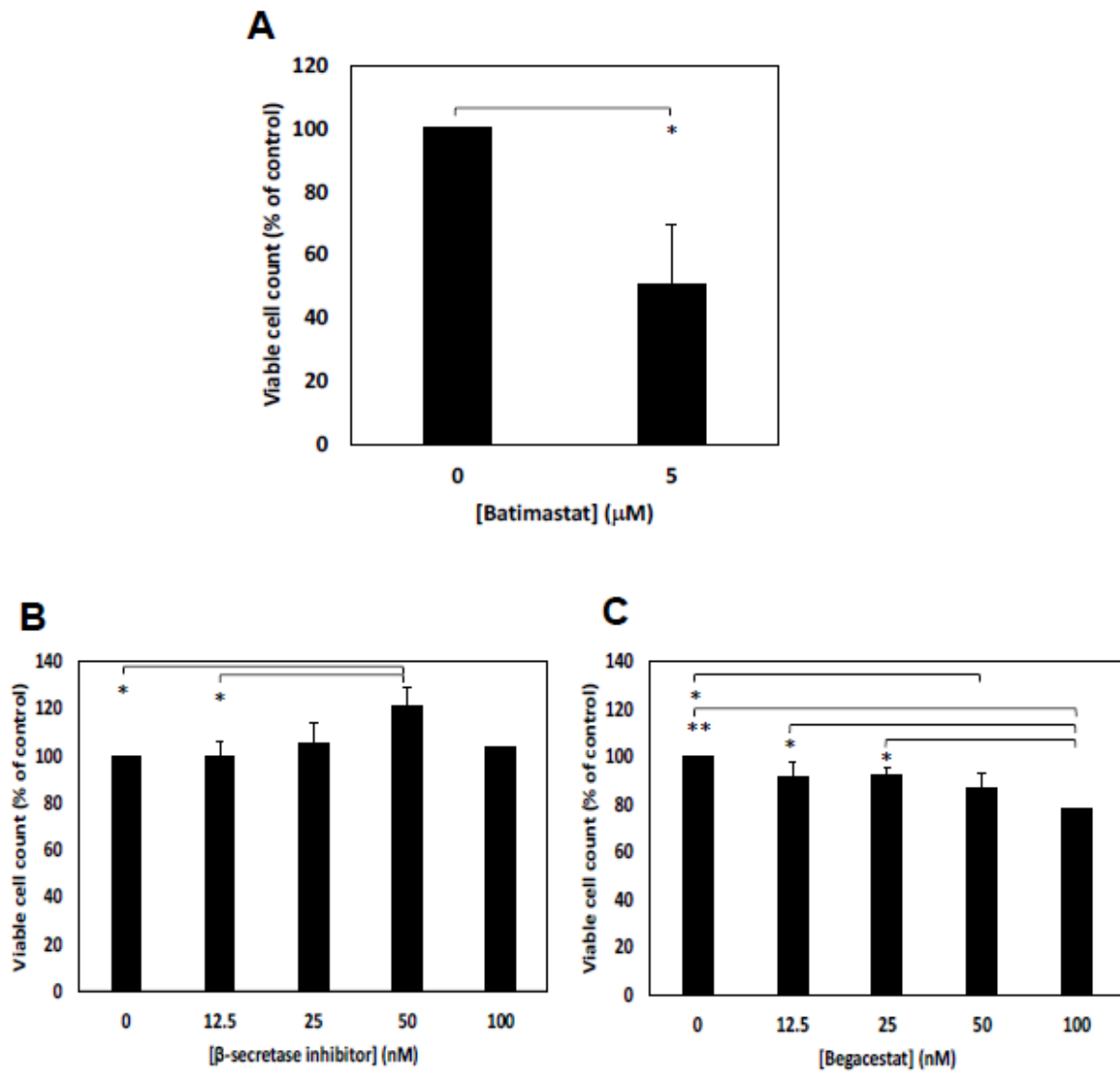


Figure 9

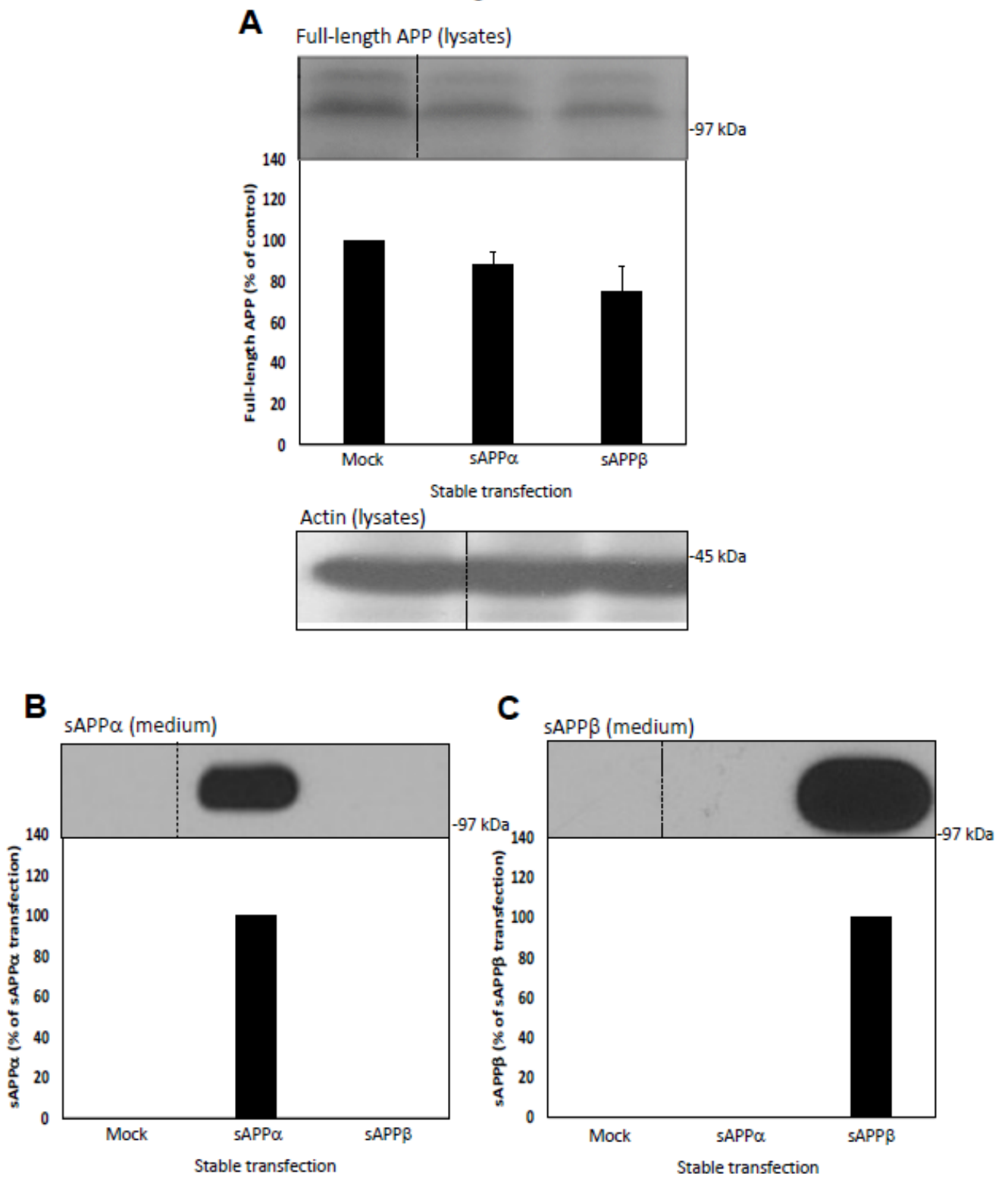


Figure 10

